Dynamics of Stiff-Chain Polymers in Isotropic Solution. 4. Multicomponent Systems

Takahiro Sato,* Atsuyuki Ohshima, and Akio Teramoto

Department of Macromolecular Science, Osaka University, Toyonaka, Osaka 560, Japan

*Received October 7, 1993; Revised Manuscript Received December 11, 1993**

ABSTRACT: As an extension of the previous work, we formulated the rotational and longitudinal diffusion coefficients (D_r and $D_\parallel$) of stiff-chain polymers in a multicomponent polymer solution. In the formulation, the stiff-chain polymer is replaced by the "fuzzy cylinder model", and a mean-field Green function method and a hole theory were used to obtain D_r and $D_\parallel$, respectively. The zero-shear viscosity η_0 for the multicomponent solution of stiff-chain polymers was calculated from D_r formulated through the η_0–D_r relation. In order to test the present theory, η_0 of quasi-ternary solutions consisting of two fractionated xanthan (a rigid double-helical polysaccharide) samples with different molecular weights and aqueous salt were measured as functions of the weight ratio of the two samples and the total polymer concentration. The experimental results were nicely reproduced by the present theory, when values of the parameters related to the jamming effect on $D_\parallel$ were suitably chosen.

1. Introduction

In a previous paper (part 3 of this series),[1] we discussed the global dynamics (the rotational and longitudinal diffusions and the zero-shear viscosity) of stiff-chain polymers in monodisperse polymer solutions of finite concentrations. In order to take into account the polymer chain flexibility effects on the global dynamics, we used the "fuzzy cylinder model" for stiff-chain polymers and extended a dynamical theory for rodlike polymer solutions to stiff or semiflexible polymer systems. Here the fuzzy cylinder model is a representation of the cylindrical distribution of polymer segments about the end-to-end vector of the polymer obtained by smearing out the positions of stiff-chain segments on condition that the position of the center of mass and the orientation of the end-to-end vector of the polymer are fixed (cf. section 2.1).

In the present study, the previous theory is extended to multicomponent solutions containing two or more stiff-chain polymer species. A Green function method for the rotational diffusion coefficient D_r and a hole theory for the longitudinal diffusion coefficient $D_\parallel$, both of which are used in the previous theory, can be straightforwardly extended to the multicomponent solution. Further the zero-shear viscosity η_0 of the multicomponent solution can be written in terms of D_r of each polymer species. These formulations are described in section 2.

Marrucci and Grizzuti[2] calculated η_0 of multicomponent rodlike polymer solutions using the Doi–Edwards tube model theory.[3-5] As mentioned previously,[1,6] the tube model theory is not valid in dilute and concentrated isotropic regimes, because in the former regime the tube enclosing the test rod can be formed only imperfectly and in the latter the jamming effect on $D_\parallel$ neglected in the theory becomes important. The present theory is free from these deficiencies and can be applied to solutions over a wide concentration region (from the dilute to concentrated isotropic region).

In order to test the present theory for global dynamics in multicomponent stiff polymer solutions, we measured η_0 of quasi-ternary solutions consisting of two fractionated xanthan samples with different molecular weights and aqueous salt as functions of the weight ratio of the two samples and the total polymer concentration. Here xanthan is a rigid double-helical polysaccharide with the persistence length of 120 nm. This polymer was chosen for the present study, because η_0 of quasi-binary solutions of fractionated xanthan samples[7] were preferably compared with the previous theory for monodisperse stiff polymer solutions.[1] The experimental details and results are described in sections 3 and 4, respectively. Section 5 compares the experimental results for η_0 with the present theory for bidisperse stiff polymer solutions.

2. Theory

2.1. Model. Let us consider an isotropic solution of r kinds of stiff-chain polymers dissolved in a low-molecular-weight solvent. We express the contour length, persistence length, and diameter of polymer species s ($1 \le s \le r$) by L_s, q_s, and d_s, respectively. In order to formulate global dynamical properties of this solution, each stiff-chain polymer molecule in the solution is replaced by a fuzzy cylinder as in the previous study.[1] The fast internal motion of the stiff chain smears the instantaneous distribution of the chain segments, and the fuzzy cylinder stands for the cylindrical distribution of segments after this smearing. Thus it follows that the effective length $L_{e,s}$ and the effective diameter $d_{e,s}$ of the fuzzy cylinder of species s are defined by the following equations:

$$L_{e,s} = \langle R_s^2 \rangle^{1/2}, \qquad d_{e,s} = [\langle [H_s(L_s/2)]^2 \rangle + d_s^2]^{1/2} \quad (1)$$

where $\langle R_s^2 \rangle$ and $\langle [H_s(L_s/2)]^2 \rangle$ are the mean-square end-to-end distance and the mean-square distance of the chain midpoint from the end-to-end displacement axis of species s, respectively. In this treatment we assume that any polymer species is so stiff that its conformation is not perturbed by the intramolecular excluded-volume effect at any concentration. In this situation both $\langle R_s^2 \rangle$ and $\langle [H_s(L_s/2)]^2 \rangle$ can be given as functions of the Kuhn statistical segment number $N_s (\equiv L_s/2q_s)$ along with q_s.[8,9]

2.2. Rotational Diffusion Coefficient. We consider first the rotational diffusion coefficient $D_{r,s}$ of a fuzzy cylinder of species s in the above multicomponent solution. Teraoka and Hayakawa[10] treated the rotational diffusion of a rod in a monodisperse rod solution by the mean-field Green function method, and in the previous paper we[1] extended their method to (monodisperse) semiflexible polymer solutions using the fuzzy cylinder model. As

* Abstract published in *Advance ACS Abstracts*, February 15, 1994.

0024-9297/94/2227-1477$04.50/0

shown in the following, this Green function method can be straightforwardly extended to the present multicomponent solutions.

Let us imagine a sphere S_t with a diameter equal to $L_{e,s}$ which just encloses a test fuzzy cylinder of species s in consideration. During the rotation the test fuzzy cylinder may collide with portions of surrounding fuzzy cylinders overlapping with this sphere S_t, and this collision slows down the rotational diffusion of the test cylinder. When the test cylinder as well as the portions of the surrounding cylinders overlapping with S_t are projected onto the surface of S_t, the rotational diffusion process of the test cylinder can be identified with the two-dimensional translational diffusion process of a round particle (the projection of the test cylinder) on the surface of S_t hindered by ribbon-like obstacles (the projections of surrounding cylinder portions).

Now we introduce the Green function $G_s(\mathbf{r},\mathbf{r}';t,t')$ associated with the diffusion equation describing this two-dimensional diffusion process of species s; the Green function has the meaning of a conditional probability that the diffusing particle at position $\mathbf{r}'$ at time t' moves to position $\mathbf{r}$ at time t. If one can obtain $G_s(\mathbf{r},\mathbf{r}';t,t')$, the effective diffusion coefficient D_s of the process during long time interval $t - t'$ can be calculated from the equation

$$D_s = \lim_{t-t'\to\infty}\left[-\frac{1}{4(t-t')}\frac{\partial^2 G_s(k;t,t')}{\partial k^2}\bigg|_{k=0}\right] \quad (2)$$

where $G_s(k;t,t')$ is the Fourier transform of the Green function $G_s(\mathbf{r},\mathbf{r}';t,t')$. According to Teraoka and Hayakawa's method,[10] we formulate this Green function and its Fourier transform. First the Green function is assumed to satisfy the following Dyson equation:

$$\langle G_s\rangle = G_{0,s} + G_{0,s}\langle\sum_{i=1}^{M} Q_i\rangle\langle G_s\rangle \quad (3)$$

where $G_{0,s}$ is the unperturbed Green function (for the free diffusion), Q_i the ith perturbation element, and M the number of the elements appearing between t and t'; the angular brackets $\langle\cdots\rangle$ denote the average with respect to the probability of the appearance and disappearance of the obstacles on the spherical surface. Repeated substitutions of the whole right-hand side of eq 3 into $\langle G_s\rangle$ in the right-hand side give the infinite series

$$\langle G_s\rangle = G_{0,s} + G_{0,s}\langle\sum_{i=1}^{M} Q_i\rangle G_{0,s} + G_{0,s}\langle\sum_{i=1}^{M} Q_i\rangle G_{0,s}\langle\sum_{j=1}^{M} Q_j\rangle G_{0,s} + \ldots \quad (4)$$

which means that $\langle G_s\rangle$ defined by eq 3 is a Green function perturbed by any numbers of sequential independent elements. $\langle G_s\rangle$ is referred to as a mean-field Green function.

Now $\langle G_s\rangle$ in eq 3 is denoted by $\langle G_{M,s}\rangle$ to indicate explicitly that this Green function is perturbed by M perturbation elements, and further new (hypothetical) Green functions defined by

$$\langle G_{m,s}\rangle = G_{0,s} + G_{0,s}\langle\sum_{i=1}^{m} Q_i\rangle\langle G_{m,s}\rangle \quad (m = 1, 2, \ldots, M) \quad (5)$$

are introduced, which pick up mean effects of m perturbation elements out of the total M elements. It can be shown that eq 5 is equivalent to the following recurrence formula:[10]

$$\langle G_{m,s}\rangle = \langle G_{m-1,s}\rangle + \langle G_{m-1,s}\rangle\langle Q_m\rangle\langle G_{m-1,s}\rangle \quad (m = 1, 2, \ldots, M) \quad (6)$$

where the last Green function in the right-hand side has been changed from $\langle G_{m,s}\rangle$ to $\langle G_{m-1,s}\rangle$, since M is a very large number. Using the method of mirror images and some mathematical manipulations, one can calculate the Fourier transform of the second perturbation terms in the right-hand side of eq 6 and obtain the recurrence formula for the effective diffusion coefficient $D_{m,s}$ corresponding to $\langle G_{m,s}\rangle$ from eq 2 given by[11]

$$\frac{D_{m,s}}{D_{0,s}} = \frac{D_{m-1,s}}{D_{0,s}} - \frac{4b}{3\pi^{1/2}S(t-t')}\tau^{3/2}D_{0,s}^{1/2}\left(\frac{D_{m-1,s}}{D_{0,s}}\right)^{3/2} \quad (7)$$

where $D_{0,s}$ is the unperturbed diffusion coefficient, b and τ the average length and the mean lifetime of the ribbon-like obstacle, respectively, and S an area comparable to the maximum range where the particle can reach by diffusion during $t - t'$.

In the case of a multicomponent solution, the above two-dimensional diffusion is perturbed by r different kinds of obstacles or perturbation elements in the diffusion space. Hereafter we explicitly distinguish the different kinds of the perturbation elements. Let M_u be the number of the perturbation elements belonging to hindering fuzzy cylinders of species u. It is convenient that each element among total $M(\equiv\sum_{u=1}^{r} M_u)$ elements is numbered in the following way: the elements of species 1 are given the numbers from 1 to M_1, the elements of species 2 are given the numbers from $(M_1 + 1)$ to $(M_1 + M_2)$, ..., and the elements of species r are given the numbers from $[(\sum_{u=1}^{r-1} M_u) + 1]$ to M. It is noted that this numbering is just to distinguish the different kinds of obstacles and has nothing to do with the order of the appearance of the obstacles in the diffusion space.

Using this numbering, we rewrite eq 7 as

$$\frac{D_{m,s}}{D_{0,s}} = \frac{D_{m-1,s}}{D_{0,s}} - \frac{4b_m^{(s)}}{3\pi^{1/2}S(t-t')}(\tau_m^{(s)})^{3/2}D_{0,s}^{1/2}\left(\frac{D_{m-1,s}}{D_{0,s}}\right)^{3/2} \quad (m = 1, 2, \ldots, M) \quad (7')$$

to express explicitly the dependence of b and τ on the kind of the obstacles by the subscript; b and τ depend also on the kind of test cylinder, which is specified by the superscript in the parentheses. This is a difference equation for $(D_{m,s}/D_{0,s})$. Since M is very large, we approximate this difference equation by the following differential equation:

$$\frac{d}{dm}\left(\frac{D_{m,s}}{D_{0,s}}\right) = -\frac{4b_m^{(s)}}{3\pi^{1/2}S(t-t')}(\tau_m^{(s)})^{3/2}D_{0,s}^{1/2}\left(\frac{D_{m,s}}{D_{0,s}}\right)^{3/2} \quad (8)$$

Since this differential equation contains the parameters $b_m^{(s)}$ and $\tau_m^{(s)}$ depending on the obstacle species, it should be integrated stepwise in the ranges of m from 0 to M_1, from M_1 to $(M_1 + M_2)$, and so on, up to the range from $(\sum_{u=1}^{r-1} M_u)$ to M. With the boundary condition $(D_{m,s}/D_{0,s}) = 1$ at $m = 0$, the first step integration gives

$$\left(\frac{D_{M_1,s}}{D_{0,s}}\right) = \left[1 + \frac{2M_1 b_1^{(s)}}{3\pi^{1/2}S(t-t')}(\tau_1^{(s)})^{3/2}D_{0,s}^{1/2}\right]^{-2}$$

and the last step integration yields the solution

$$\frac{D_s}{D_{0,s}} \equiv \frac{D_{M,s}}{D_{0,s}} = \left[1 + \frac{2}{3\pi^{1/2}} \sum_{u=1}^{r} \rho_{B,u}^{(s)} b_u^{(s)} (\tau_u^{(s)})^{3/2} D_{0,s}^{1/2}\right]^{-2} \quad (9)$$

where $\rho_{B,u}^{(s)}$ [$=M_u/S(t-t')$] is the number of obstacles of species u appearing per unit area and per unit time.

Using the relation of the rotational diffusion coefficient $D_{r,s}$ ($D_{r0,s}$) of the fuzzy cylinder of species s to the two-dimensional translational diffusion coefficient D_s ($D_{0,s}$) in eq 9, i.e., $D_{r,s} = D_s/(L_{e,s}/2)^2$ ($D_{r0,s} = D_{0,s}/(L_{e,s}/2)^2$), we obtain

$$\frac{D_{r,s}}{D_{r0,s}} = \left[1 + \frac{2}{3\pi^{1/2}} \sum_{u=1}^{r} \rho_{Br,u}^{(s)} \theta_u^{(s)} (\tau_u^{(s)})^{3/2} D_{r0,s}^{1/2}\right]^{-2} \quad (10)$$

where $\rho_{Br,u}^{(s)}$ ($\equiv \rho_{B,u}^{(s)}(L_{e,s}/2)^2$) is the number of ribbon-like obstacles of species u (on the surface of S_t enclosing the fuzzy cylinder of species s) per unit solid angle and per unit time, and $\theta_u^{(s)}$ ($\equiv b_u^{(s)}/(L_{e,s}/2)$) is the average central angle subtended by the ribbon-like obstacles.

Our next task is to express the quantities $\rho_{Br,u}^{(s)}$, $\theta_u^{(s)}$, and $\tau_u^{(s)}$ in eq 10 in terms of molecular parameters. Since the appearance and disappearance of ribbon-like obstacles on the surface of S_t are caused predominantly by the longitudinal diffusion of the hindering cylinder or the test cylinder, we assume that $\tau_u^{(s)}$ is proportional to the shorter of the longitudinal diffusion times of the hindering and test cylinders traveling a distance of their cylinder lengths:

$$\tau_u^{(s)} \propto \begin{cases} L_{e,u}^2/D_{\parallel,u} & (L_{e,u} < L_{e,s}) \\ L_{e,s}^2/D_{\parallel,s} & (L_{e,u} \geq L_{e,s}) \end{cases} \quad (11)$$

When a surrounding cylinder contacts S_t on its periphery, the corresponding ribbon-like obstacle may disappear by a conformation change or a short-distance transverse diffusion of the hindering and/or test cylinders. The lifetime of such an obstacle should be much shorter than that expected from eq 11. Therefore, the surrounding cylinders contacting S_t on its periphery should not be counted as hindering cylinders. We assume that the fuzzy cylinder of species u becomes a hindering cylinder only when the cylinder axis comes closer to the sphere S_t than the distance $d_{c,u}/2$. The distance $d_{c,u}$ is a parameter ranging from 0 to $d_{e,u}$ which is not determined *a priori*; it may be called the core diameter of the hindering cylinder.

The quantity $\rho_{Br,u}^{(s)}$ is proportional to $v_{ex}c_u'/\tau_u^{(s)}$ where v_{ex} is the mutual excluded volume between the hindering cylinder core of species u and the sphere S_t and c_u' the number concentration of species u; v_{ex} is given by[12]

$$v_{ex} = \frac{\pi}{4} L_{e,s}^2 \left(L_{e,u} + \frac{2}{3} L_{e,s}\right) f_r\left(\frac{d_{c,u}}{L_{e,s}}, \frac{d_{c,u}}{3L_{e,u} + 2L_{e,s}}\right) \quad (12)$$

with a finite-thickness correction factor for the hindering cylinder

$$f_r(x_1,x_2) = (1 + x_1)^2(1 - x_2) \quad (13)$$

(Equation 13 was obtained on the assumption that the core of the hindering cylinder is a spherocylinder.) The angle $\theta_u^{(s)}$ should increase with increasing $L_{e,u}$ at $L_{e,u} < L_{e,s}$ and become constant at $L_{e,u} \geq L_{e,s}$, so that it may be written as

$$\theta_u^{(s)} \propto \begin{cases} L_{e,u}/L_{e,s} & (L_{e,u} < L_{e,s}) \\ 1 & (L_{e,u} \geq L_{e,s}) \end{cases} \quad (14)$$

Substitution of eqs 11–14 into eq 10 yields

$$\frac{D_{r,s}}{D_{r0,s}} = \left[1 + \beta_r^{-1/2} \frac{L_{e,s}}{L_s} \left(\frac{F_\parallel(p_s,N_s)}{F_r(p_s,N_s)}\right)^{1/2} \sum_{u=1}^{r} c_u' L_{e,u}^3 \left(\frac{3}{5} + \frac{2}{5}\frac{L_{e,s}}{L_{e,u}}\right) f_r\left(\frac{d_{c,u}}{L_{e,s}}, \frac{d_{c,u}}{3L_{e,u} + 2L_{e,s}}\right) H_{su}'\right]^{-2} \quad (15)$$

with

$$H_{su}' \equiv \begin{cases} \left(\frac{L_u F_\parallel(o_u,N_u)}{L_s F_\parallel(p_s,N_s)}\right)^{1/2} \left(\frac{D_{\parallel 0,u}}{D_{\parallel,u}}\right)^{1/2} & (L_{e,u} < L_{e,s}) \\ \left(\frac{L_{e,s}}{L_{e,u}}\right)^2 \left(\frac{D_{\parallel 0,s}}{D_{\parallel,s}}\right)^{1/2} & (L_{e,u} \geq L_{e,s}) \end{cases} \quad (16)$$

where L_s is the contour length of the wormlike chain species s and β_r is the proportional constant which was estimated by Teraoka et al.[13] to be 1350. In the above equations, we have used the relation

$$D_{\parallel 0,s} = \frac{1}{6} L_s^2 D_{r0,s} [F_r(p_s,N_s)/F_\parallel(p_s,N_s)] \quad (17)$$

where $F_r(p_s,N_s)$ and $F_\parallel(p_s,N_s)$ are finite-thickness and flexibility correction factors associated with $D_{r0,s}$ and $D_{\parallel 0,s}$, respectively, which are given by eqs A7 and A12 in ref 1; p_s and N_s are the axial ratio and the Kuhn segment number of the wormlike chain of species s, respectively.

2.3. Longitudinal Diffusion Coefficient. Equation 16 contains the longitudinal diffusion coefficient $D_\parallel$ of the fuzzy cylinder or the stiff polymer chain at finite concentration, and thus next we must formulate $D_\parallel$. In a considerably concentrated solution, the stiff polymer chain must be hindered by surrounding chains from the longitudinal diffusion motion and may be released from the hindrance not only by the longitudinal diffusion of the hindering chain but also by the local conformation changes of the hindering and test chains. Although Edwards and Evans[14] and also we[6] proposed Green function methods to formulate $D_\parallel$ for rodlike polymers in concentrated solution, these methods took into account only the former release mechanism; it is difficult to incorporate the latter release mechanism for polymers with flexibility into the Green function methods. In the previous study,[1] we have used a hole theory similar to the Cohen–Turnbull theory[15] for the self-diffusion in low molar mass liquids to obtain an expression of $D_\parallel$ in monodisperse stiff-chain polymer solutions. Here we apply this hole theory to the multicomponent stiff-chain polymer system.

In the previous theory,[1] the longitudinal diffusion of the stiff-chain or fuzzy cylinder is assumed to occur effectively only when a "hole" (i.e., solvent domain) larger than a critical hole appears in front of the cylinder, and thus $D_\parallel$ is proportional to the probability of finding a hole which is larger than the critical hole. This probability obeys the Poisson distribution and can be written with the mutual excluded volume $V_{ex,u}^{*(s)}$ between the critical hole for the diffusing chain of species s and the hindering polymer chain of species u. The final result is given by

$$\frac{D_{\parallel,s}}{D_{\parallel 0,s}} = \exp\left[-\sum_{u=1}^{r} V_{ex,u}^{*(s)} c_u'\right] \quad (18)$$

where $D_{\parallel 0,s}$ is the longitudinal diffusion coefficient for species s at infinite dilution.

Although the critical hole should be related to the hindering and release processes of the longitudinal dif-

fusion, this relation has not been established yet. In the previous study,[1] we simply assumed that the critical hole is similar to the diffusing fuzzy cylinder and the similtude ratio λ^* is independent of the polymer molecular weight. This assumption was demonstrated to describe well the experimental results of the zero-shear viscosity for some quasi-binary stiff polymer solutions.[1] Using the same assumption, we write the excluded volume $V_{ex,u}^{*(s)}$ as

$$V_{ex,u}^{*(s)} = V(\lambda_u^{*(s)}L_{e,s}, \lambda_u^{*(s)}d_{e,s}; L_u, d_u) \tag{19}$$

with

$$V(L_1,d_1;L_2,d_2) \equiv \frac{\pi}{4}\Big[L_1L_2(d_1+d_2) + L_1d_1^2 + L_2d_2^2 + \frac{1}{2}(L_1d_2^2 + L_2d_1^2) + \frac{\pi}{2}(L_1+L_2)d_1d_2 + \frac{\pi}{4}d_1d_2(d_1+d_2)\Big] \tag{20}$$

and $\lambda_u^{*(s)}$ is the similitude ratio of the critical hole to the diffusing fuzzy cylinder. Since the hindering and release processes of the longitudinal diffusion occur in corporation of the diffusing and hindering polymers, $\lambda_u^{*(s)}$ should depend on both polymer species; the super- and subscripts are attached to the similitude ratio $\lambda_u^{*(s)}$ to specify the species of diffusing polymer (the superscript) and the species of hindering polymer (the subscript). The similitude ratios should be taken as adjustable parameters in our theory.

2.4. Zero-Shear Viscosity. In general, the shear stress in a polymer solution is induced not only by the end-over-end rotational motion of each polymer chain in the solution but also by its more faster internal motions. However, at a sufficiently low shear rate, the contribution of the end-over-end rotational motion overwhelms those of the internal motions, so that the shear stress at a low shear rate (or the zero-shear viscosity η_0) of the solutions may be related to the end-over-end rotational diffusion coefficient D_r of the polymer chain.

In the previous study,[1] we slightly modified Doi–Edwards' zero-shear viscosity expression[5] for rodlike polymer solutions by incorporating finite thickness effects of the polymer and used it for monodisperse stiff polymer solutions. This expression can be straightforwardly extended to the multicomponent polymer solutions:

$$\eta_0 = \eta_{solv} + \sum_{s=1}^{r}\left[(4\gamma_s^{-1} - 3\chi_s^2)\frac{c_s'k_BT}{30D_{r0,s}} + \chi_s^2\frac{c_s'k_BT}{10D_{r,s}}\right] \tag{21}$$

where η_{solv} is the solvent viscosity, γ_s and χ_s are two finite thickness correction factors, k_B is the Boltzmann constant, and T is the absolute temperature; the first and second terms in the brackets of eq 21 correspond to the hydrodynamic energy dissipation due to the friction between the polymer and solvent and the orientational entropy loss of the chain under the shear flow, respectively. Since the intrinsic viscosity $[\eta]_s$ of the polymer species s can be related to $D_{r0,s}$ by

$$[\eta]_s c w_s = \frac{2c_s'k_BT}{15\gamma_s\eta_{solv}D_{r0,s}} \tag{22}$$

eq 21 can be rewritten in the form

$$\frac{\eta_{sp}}{c} = \sum_{s=1}^{r} w_s[\eta]_s\left(1 - \frac{3}{4}\gamma_s\chi_s^2 + \frac{3}{4}\gamma_s\chi_s^2\frac{D_{r0,s}}{D_{r,s}}\right) \tag{23}$$

where c is the total polymer mass concentration, w_s the weight fraction of the polymer species s in the whole polymer components, and η_{sp} the specific viscosity $[\equiv(\eta_0 - \eta_{solv})/\eta_{solv}]$. In eq 23 the ratio $D_{r0,s}/D_{r,s}$ can be calculated using eq 15; the two correction factors γ_s and χ_s can be estimated from equations given in appendices of ref 1.

Table 1. Molecular Characteristics of Xanthan Samples Used

sample	species	$[\eta]/(cm^3\ g^{-1})$	$M_v/10^4$	L/nm	N
S-4-5-2	1	194	25	129	0.54
R-6p	2	2765	208	1070	4.5

3. Experimental Section

In part 2 of this series,[7] zero-shear viscosities η_0 of aqueous solutions containing a single fractionated xanthan sample and sodium chloride (NaCl) as an added salt were measured as a function of the concentration and molecular weight of the polymer. Here xanthan is a rigid double-helical ionic polysaccharide with a persistence length of ca. 120 nm.[16] The present study has extended the same measurements to aqueous solutions with two fractionated xanthan samples with different molecular weights and NaCl.

Two xanthan samples R-6p and S-4-5-2 used for the viscosity measurement were sonicated, purified, fractionated, and converted to the sodium salt form by the established method. Table 1 shows molecular characteristics of both samples. Here $[\eta]$ is the intrinsic viscosity in 0.1 M aqueous NaCl at 25 °C, M_v is the viscosity-average molecular weight estimated using the reported $[\eta]$–weight-average molecular weight relation,[16] and L and N are the contour length and the number of the Kuhn statistical segments, respectively, both of which were calculated from M_v using the molar mass per unit contour length $M_L = 1940\ nm^{-1}$ and the persistence length $q = 120$ nm.[16] In what follows, the lower (S-4-5-2) and higher (R-6p) molecular weight samples are denoted by species 1 and 2, respectively.

Mixtures of the samples R-6p and S-4-5-2 with the weight fraction w_2 of the higher molecular weight sample (R-6p) were dissolved in 0.1 M aqueous NaCl to make a "quasi-ternary solution" with the total polymer mass concentration c and were used for the following viscosity measurements. As reference, viscosity measurements were also made for "quasi-binary solutions" containing only the single sample either R-6p or S-4-5-2 as a function of the polymer concentration c.

Viscosities η of concentrated isotropic solutions above ca. 0.1 Pa s were measured at several (apparent) shear rates by a magnetically-controlled suspending-ball rheometer.[17] The test solution was put in a stoppered test tube where solvent evaporation from the solution was minimized. The temperature of the test solution was controlled at 25 °C by thermostated circulating water. The zero-shear viscosity η_0 of each solution was determined by extrapolating η obtained to zero-shear rate. Solution viscosities below 0.1 Pa s were measured by a low-shear four-bulb capillary viscometer at 25 °C and extrapolated to the zero-shear rate. (The same type of viscometer was also used to determine $[\eta]$ of sample R-6p.)

4. Results

In Figure 1, the results of η_0 obtained for quasi-binary solutions of R-6p and S-4-5-2 are plotted against the polymer mass concentration c double logarithmically by circles. Similar to the results in part 2,[7] η_0 of the quasi-binary solutions sharply increases with increasing c at high c, and the concentration dependence does not obey any power law. On the other hand, the triangles in Figure 1 show η_0 for quasi-ternary solutions containing the two samples R-6p and S-4-5-2 with three different polymer compositions w_2 as functions of the total polymer mass concentration c. The total polymer concentration dependence of η_0 for the quasi-ternary solutions has a trend similar to that of the quasi-binary solutions, although there are no data points at lower c.

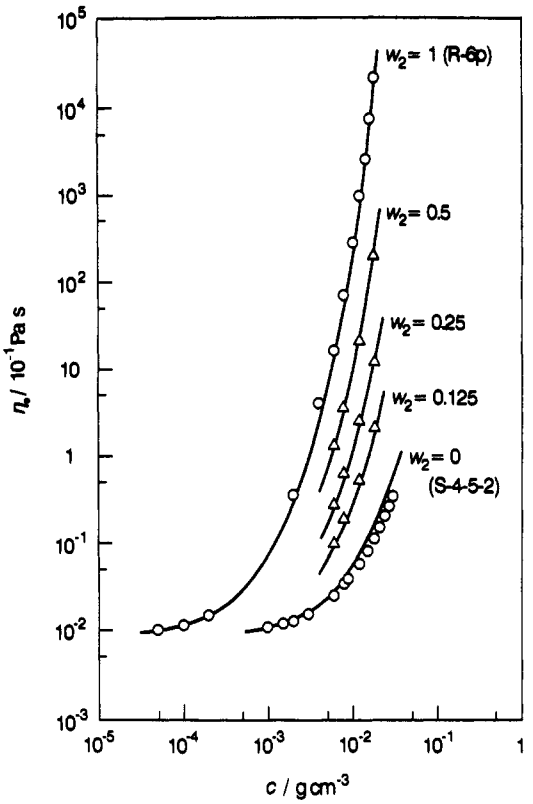

Figure 1. Double-logarithmic plot of the zero-shear viscosity η_0 vs the (total) polymer mass concentration c for quasi-binary and quasi-ternary aqueous solutions of xanthan with 0.1 M sodium chloride: circles, quasi-binary solutions; triangles, quasi-ternary solutions; curves, calculated from the present and previous theories for bidisperse and monodisperse stiff polymer solutions (see section 5).

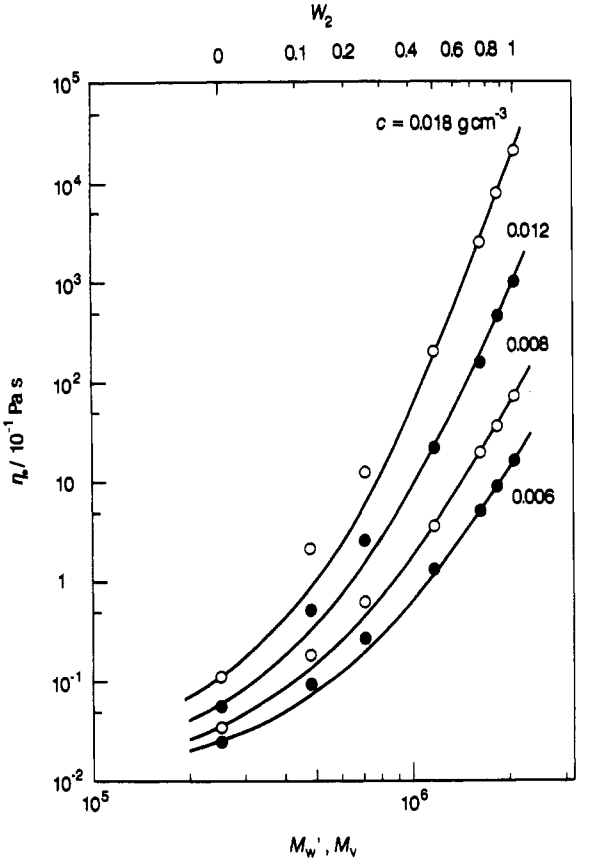

Figure 2. Double-logarithmic plot of η_0 for quasi-ternary xanthan solutions with fixed c against the "weight-average molecular weight" M_w' calculated from eq 24: circles, results for quasi-ternary solutions; curves, η_0–M_v relations for quasi-binary solutions obtained from the previous study.[7]

It is known that η_0 for polydisperse *flexible* polymer solutions is almost determined by the weight-average molecular weight.[18] We examine whether this empirical blending law is valid also for the present xanthan solutions or not. Since M_v of our xanthan samples should be close to the (true) weight-average molecular weight, we may calculate "the weight-average molecular weight" M_w' for the xanthan mixture in quasi-ternary solutions by the equation

$$M_w' \equiv (1 - w_2)M_{v,1} + w_2 M_{v,2} \tag{24}$$

where $M_{v,1}$ and $M_{v,2}$ are the viscosity-average molecular weights of the shorter species 1 (S-4-5-2) and the longer species 2 (R-6p), respectively. In Figure 2, circles show the M_w' dependence of η_0 for quasi-ternary solutions with fixed c, whereas solid curves represent the η_0–M_v relations for quasi-binary solutions of xanthan with the solvent condition and polymer concentrations the same as those of the ternary solutions, which are obtained by the interpolation of η_0 data in part 2[7] to the given concentrations.

The circles for the quasi-ternary solutions almost follow the solid curves for the quasi-binary solutions with the same c at a higher M_w' or larger w_2 region (cf. the upper axis of Figure 2). However, appreciable upward deviations of the data points from the curves are observed at a smaller w_2 region. This indicates imperfectness of the above-mentioned empirical blending law for the present stiff-chain polymer system. In other words, the weight-average molecular weight is not a suitable parameter to analyze η_0 data for solutions of a polydisperse stiff polymer with a higher molecular weight tail. We need some other blending law for stiff-chain polymer solutions. In the next section, the η_0 data for the quasi-ternary xanthan solutions are compared with the molecular theory described in section 2 in place of the empirical blending law.

5. Comparison between Experiment and Theory

In part 3 of this series,[1] η_0 for quasi-binary solutions of xanthan, as well as of another rigid polysaccharide schizophyllan, are favorably compared with the fuzzy cylinder model theory for monodisperse polymer systems. In that comparison, the similitude ratio λ^* of the critical hole for longitudinal diffusion to the fuzzy cylinder (cf. section 2.3) was chosen to be 0.11 for xanthan. Using the same value of λ^*, the fuzzy cylinder model theory for monodisperse polymers (indicated by the top and bottom solid curves in Figure 1) can almost fit the data points for η_0 of quasi-binary solutions of both samples R-6p and S-4-5-2. The core diameter d_c of the fuzzy cylinder (cf. section 2.2) for both xanthan samples was chosen to be zero, which is consistent with the previous results in part 3 (cf. Figure 6 in ref 1).

Next we compare the results of η_0 for quasi-ternary solutions with the fuzzy cylinder model theory described in section 2. Figure 3 shows the polymer composition dependence of the reduced viscosity η_{sp}/c for quasi-ternary solutions of xanthan with the total polymer concentration c = 0.018 g/cm^3; the circles represent the values of η_{sp}/c calculated from the data in Figure 2 for the same c. On the other hand, the dashed curve in Figure 3 is calculated on the assumption that each xanthan molecule of species s (s = 1, 2) in the ternary solution with c (the total polymer concentration) and w_s (the weight fraction of species s in the total polymer) does not interact with molecules of the other species. In such a case, the rotational and longi-

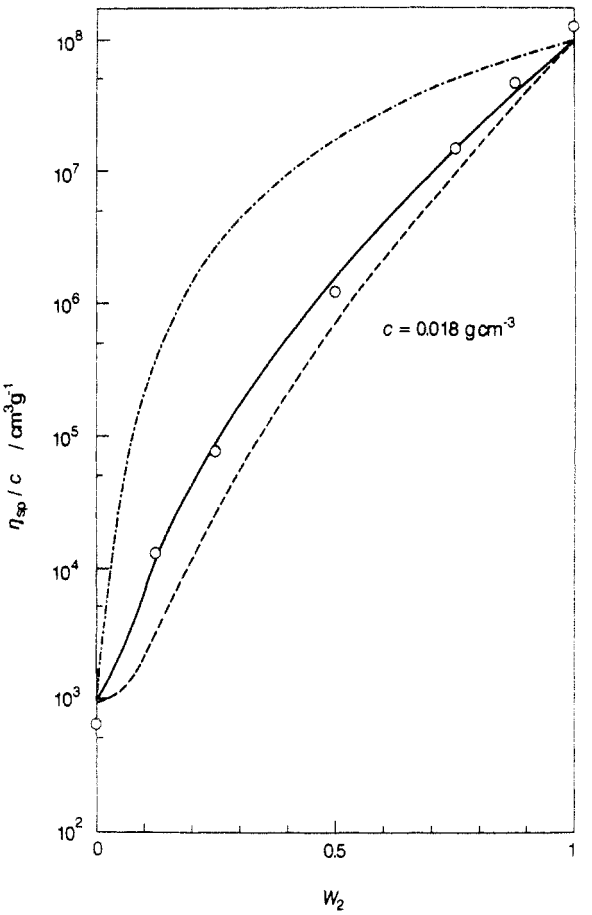

Figure 3. Polymer composition dependence of the reduced viscosity η_{sp}/c for aqueous xanthan solutions with the total polymer concentration c = 0.018 g cm^{-3}: circles, experimental data; dashed curve, calculated on the assumption that the polymer does not affect the diffusion motion of the polymer of the different species (see text); solid and dot-dash curves, calculated from the present theory using $(\lambda_1^{*(1)},\lambda_1^{*(2)},\lambda_2^{*(1)},\lambda_2^{*(2)})$ = (0.11, 0.058, 0.11, 0.11) and (0.11, 0.11, 0.11, 0.11), respectively.

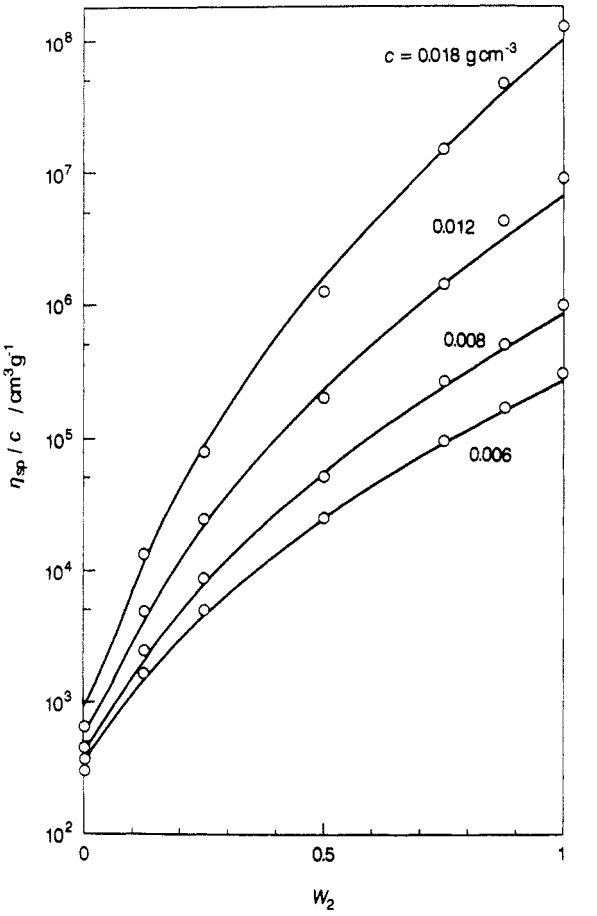

Figure 4. Comparison between theory and experiment for quasi-ternary solutions of xanthan with different total polymer concentrations: circles, experimental data; curves, calculated using $(\lambda_1^{*(1)},\lambda_1^{*(2)},\lambda_2^{*(1)},\lambda_2^{*(2)})$ = (0.11, 0.058, 0.11, 0.11).

tudinal diffusion coefficients of species s should be equal to those in the binary solution with the polymer mass concentration cw_s, and the reduced viscosity η_{sp}/c may be calculated from eq 23 with $D_{r0,s}/D_{r,s}$ from the fuzzy cylinder model theory for monodisperse polymer systems used just above. The dashed curve appreciably deviates downward from the experimental data points. This deviation manifests itself in the contribution of the interspecies interaction to the rotational and longitudinal diffusion motions of each polymer molecule.

In order to calculate η_{sp}/c from the fuzzy cylinder model for bidisperse polymer systems, we have to determine the values of four similitude ratios $\lambda_1^{*(1)}$, $\lambda_2^{*(2)}$, $\lambda_1^{*(2)}$, and $\lambda_2^{*(1)}$. Here $\lambda_u^{*(s)}$ represents how efficiently the longitudinal diffusion of species s is hindered by a molecule of species u (cf. eqs 18–20). Since the hindrance of the longitudinal diffusion by a molecule of the same species in a bidisperse polymer system should be the same as that in the corresponding monodisperse system, we can assume $\lambda_1^{*(1)}$ and $\lambda_2^{*(2)}$ for xanthan in quasi-ternary solutions to be 0.11. On the other hand, the efficiency of the hindrance by a molecule of dissimilar species may not be the same as that by a molecule of the same species, because the hindering and release processes of the longitudinal diffusion occur in cooperation between the hindering and diffusing chains. Therefore, $\lambda_1^{*(2)}$ and $\lambda_2^{*(1)}$ cannot be necessarily assumed to be the same as $\lambda_1^{*(1)}$ and $\lambda_2^{*(2)}$.

With $\lambda_1^{*(1)}$ and $\lambda_2^{*(2)}$ fixed to 0.11, we searched for values of $\lambda_1^{*(2)}$ and $\lambda_2^{*(1)}$ leading to the best fit of our viscosity data to the present fuzzy cylinder model theory. When the values of $\lambda_1^{*(2)}$ and $\lambda_2^{*(1)}$ are chosen, respectively, to be 0.058 and 0.11, the theoretical curve can satisfactorily fit the experimental data points, as shown by the solid curve in Figure 3. This successful fitting confirms the previous conclusion that the fuzzy cylinder is a suitable model to describe the dynamics of stiff-chain polymers in isotropic solutions with finite concentration.

If both $\lambda_1^{*(2)}$ and $\lambda_2^{*(1)}$ are chosen to be 0.11, the theory gives the dot-dash curve in Figure 3. This curve apparently deviates upward from the experimental data points. This deviation indicates that the longer chain is hindered by the shorter chain less effectively than that by the longer chain or it is released from the hindrance by the shorter chain easier than from the hindrance by the longer chain. It is noted that η_{sp}/c is insensitive to the choice of the $\lambda_2^{*(1)}$ value. This is due to a smaller contribution of the shorter species 1 to the viscosity. Therefore, the choice of 0.11 for $\lambda_2^{*(1)}$ in Figure 3 is rather arbitrary.

Figure 4 shows the same comparison as Figure 3 for different total polymer concentrations. With $\lambda_1^{*(1)}$ = $\lambda_2^{*(2)}$ = $\lambda_2^{*(1)}$ = 0.11 and $\lambda_1^{*(2)}$ = 0.058, the agreement between theory and experiment is satisfactory for the all c. Further the curves fitting the triangles in the double-logarithmic plot of η_0 vs c of Figure 1 are the theoretical curves drawn with the same parameters. The agreement is demonstrated also in this plot.

References and Notes

(1) Sato, T.; Takada, Y.; Teramoto, A. *Macromolecules* **1991**, *24*, 6220.
(2) Marrucci, G.; Grizzuti, N. *J. Polym. Sci., Polym. Lett. Ed.* **1983**, *21*, 83.
(3) Doi, M.; Edwards, S. F. *J. Chem. Soc., Faraday Trans. 2* **1978**, *74*, 560.
(4) Doi, M.; Edwards, S. F. *J. Chem. Soc., Faraday Trans. 2* **1978**, *74*, 918.
(5) Doi, M.; Edwards, S. F. *The Theory of Polymer Dynamics*; Clarendon Press: Oxford, 1986.
(6) Sato, T.; Teramoto, A. *Macromolecules* **1991**, *24*, 193.
(7) Takada, Y.; Sato, T.; Teramoto, A. *Macromolecules* **1991**, *24*, 6215.
(8) Kratky, O.; Porod, G. *Recl. Trav. Chim. Pays-Bas* **1949**, *68*, 1106.
(9) Hoshikawa, H.; Saito, N.; Nagayama, K. *Polym. J.* **1975**, *7*, 79.
(10) Teraoka, I.; Hayakawa, R. *J. Chem. Phys.* **1989**, *91*, 2643; **1988**, *89*, 6989.
(11) This equation is for the two-dimensional diffusion of the round particle on the plane tangent to the sphere S_t, so that, strictly speaking, it should be applied for a short-time diffusion. However, as shown by Teraoka and Hayakawa,[10] the application of eq 7 to a long-time diffusion is also a good approximation.
(12) Onsager, L. *Ann. N.Y. Acad. Sci.* **1949**, *51*, 627.
(13) Teraoka, I.; Ookubo, N.; Hayakawa, R. *Phys. Rev. Lett.* **1985**, *55*, 2712.
(14) Edwards, S. F.; Evans, K. E. *J. Chem. Soc., Faraday Trans. 2* **1982**, *78*, 113.
(15) Cohen, M. H.; Turnbull, D. *J. Chem. Phys.* **1959**, *31*, 1164.
(16) Sato, T.; Norisuye, T.; Fujita, H. *Macromolecules* **1984**, *17*, 2696.
(17) Takada, Y.; Sato, T.; Einaga, Y.; Teramoto, A. *Bull. Inst. Chem. Res., Kyoto Univ.* **1988**, *66*, 212.
(18) Ferry, J. D. *Viscoelastic Properties of Polymers*, 3rd ed.; John Wiley & Sons: New York, 1980; p 515.